

The mechanism of nonlinear microwave behaviour in high- T_c superconducting devices

P Lahl and R Wördenweber

ISG and CNI, Forschungszentrum Jülich, 52425 Jülich, Germany

Received 10 November 2003

Published 14 April 2004

Online at stacks.iop.org/SUST/17/S369

DOI: 10.1088/0953-2048/17/5/056

Abstract

First, this paper gives an overview of possible origins and mechanisms that might be responsible for experimentally observed nonlinear effects. Focusing on well-known physical loss mechanisms with nonlinear characteristics, their impact on microwave properties and their relevance in microwave devices are discussed. Secondly, an experimental investigation of the power handling capability of coplanar resonators in additionally applied dc magnetic fields in zero field cooled, field cooled, and field sweep experiments is presented. These experiments demonstrate that the microwave power handling capability of optimized high- T_c thin film devices is limited by a maximum current density, and suggest that the limitation is caused by the dc critical current density J_c of the superconducting material.

1. Introduction

The application of superconductivity in thin film microwave devices often implies large power densities. Nonlinear effects limit the power handling capability of the devices. Due to their intrinsic and extrinsic properties, superconductors convey new limiting mechanisms compared to normal conducting materials. Considerable effort has been invested worldwide to uncover the *fundamental* nonlinear mechanisms responsible for the observed nonlinear effects. Such nonlinear effects include, for example, microwave power dependent losses represented by a nonlinear surface resistance, and the generation of harmonics and intermodulation signals. Depending on the specific device, one of these effects might receive the most attention. However, it is obvious that as soon as a nonlinearity is present, all these nonlinear effects will arise, as has been experimentally demonstrated [1–5].

Although various potential physical origins for the nonlinearities are being discussed, the fundamental physical mechanism that will ultimately define the power handling capability—if all extrinsic mechanisms have been eliminated—is not understood. In this paper, first, mechanisms that are known to limit the dc and rf performance of high- T_c superconducting material are reviewed. Then experimental results are presented that demonstrate that

- (i) the limiting mechanism in optimized high- T_c thin film microwave devices is current-driven, and

- (ii) that the limiting current density for zero field can be identified as the dc critical current density.

2. Nonlinear mechanisms

In the discussion of possible nonlinear mechanisms, we will concentrate on those mechanisms which can be considered fundamental. In this sense heating effects, for example, are secondary mechanisms that may be generated by any loss mechanism.

From a dc perspective, there exist three major nonlinear mechanisms which can be considered fundamental: (i) Cooper pair-breaking, (ii) vortex unpinning and motion, and (iii) Josephson junction behaviour. Each mechanism is associated with a maximum limiting critical current density and the mechanism with the lowest current density naturally will define the onset of nonlinear behaviour. Therefore, in the dc case, dissipation due to pair breaking can hardly be measured, since vortex unpinning and motion will occur at much smaller current densities. Furthermore, a sample with a significant amount of weak links will show dissipation at very low critical currents characterizing the weak links. In the following we will briefly review these nonlinear mechanisms and their potential relevance to rf devices.

2.1. The pair-breaking mechanism

The microwave surface resistance R_s of a superconductor is usually expressed in terms of the classical two fluid model:

$R_s = 0.5 \mu_0^2 \omega^2 \sigma_n \lambda^3$. A possible source of nonlinearity is then given by the quasi-particle density n_{qp} . In the case of a current density of the order of magnitude of the pair-breaking current density $J_{c,PB}$, n_{qp} is no longer constant, but depends strongly upon the applied current. A nonlinearity based on this effect has been predicted and investigated using a phenomenological expression for a nonlinear penetration depth $\lambda(T, j/j_{IMD}(T))$ with the phenomenological parameter $j_{IMD}(T)$ [6, 7]. Here, s- and d-wave superconductors can be distinguished since for the d-wave, excitations are in principle possible down to $j \rightarrow 0$. Applying this model to measurements, j_{IMD} can be extracted and should provide values of the order of the pair-breaking critical current density, i.e., $j_{IMD} \approx j_{c,PB}$. However, the values obtained for j_{IMD} are considerably smaller than $j_{c,PB}$. While for $j \rightarrow 0$, the d-wave nature of high temperature superconductors (HTSs) seems to show in the extremely sensitive intermodulation distortion experiments [8], Dahm *et al* conclude that pair breaking is not the mechanism that limits the power handling capability in the limit $j \rightarrow \infty$ [9]. However, although pair-breaking critical current densities are usually not reached in real systems, $j_{IMD} = j_{c,PB}$ defines an upper limit for the power handling capability of devices [10].

2.2. The vortex motion model

In type-II superconductors the observed dc critical current density is generally not defined by the pair-breaking mechanism, but instead it is limited by the 1–2 orders of magnitude smaller critical current density j_c defined by the onset of vortex motion. This critical current density is characterized by a linear dependence on temperature $J_c = J_{c,0}(1 - T/T_c)$ and values of the order 10^6 A cm⁻² at 77 K for epitaxial YBa₂Cu₃O₇ (YBCO) thin films in the limit of zero applied magnetic field [11]. Vortices may, for example, be frozen in during the cooling-down process, generated by the magnetic component of the applied dc or rf fields, or vortex–antivortex pairs may be generated due to fluctuations and broken up thermally or induced by dc or rf currents, producing free vortices. These vortices automatically produce losses due to vortex motion if the local current density exceeds j_c . Thus, vortex motion has to be considered as a nonlinear mechanism in the rf case. In the second part of this paper, we will experimentally investigate the impact of vortices on the microwave properties by investigating the nonlinear behaviour of coplanar microwave resonators in additionally applied small magnetic fields.

2.3. The Josephson junctions model

It has been shown that the linear microwave properties of highly granular high- T_c superconductors (HTSs)—especially the large surface resistances compared to single crystals—can be explained by the difference in morphology. The polycrystalline samples can be modelled by an array of Josephson junctions in the linear regime [12]. Nonlinear behaviour is expected at rf current densities which exceed the average critical current density of the constituting Josephson junctions $j_{c,JJ}$. For comparison, it has been shown that bicrystal grain boundaries with misorientation angles of $\theta > 5^\circ$ lead to a reduced dc critical current density compared to the bulk

value [13]. Accordingly, the nonlinear microwave behaviour of granular HTSs can be described by Josephson-vortex motion at moderate rf power levels and by penetration of Josephson vortices into the junctions at larger rf power levels [14–16]. The impact of grain boundaries on the rf properties have been investigated using a $\lambda/2$ microstrip resonator which contains a bicrystal grain boundary Josephson junction of various misorientation angles θ [17]. It was found that the power handling capability is only reduced from values for the overall epitaxial film by grain boundaries with misorientation angles of $\theta > 5^\circ$. These results agree nicely with the dc results. Similar observations are reported for IMD measurements [18].

Thus, although bicrystal grain boundaries are different from natural grain boundaries [19], these investigations are a strong indication that

- (i) grain boundaries determine the power handling capability in granular superconductors with misorientation angles of $\theta > 5^\circ$, and
- (ii) assuming that epitaxial thin films do not contain large-angle grain boundaries, the Josephson junction model does not represent the ultimate fundamental nonlinear mechanism for perfect high- T_c microwave devices [17].

3. Local analysis of the power handling capability via vortices

As we have discussed above, both pair-breaking and grain boundary Josephson junctions do not seem to represent the fundamental limiting mechanisms. Thus, the interesting question remains: what mechanism is responsible for the nonlinear behaviour in optimized, weak-link free thin film devices? For this purpose we examined the nonlinear properties of coplanar resonators which are ‘ideal’ in the sense that (i) they exhibit a small power handling capability so that thermal effects can be neglected, and (ii) epitaxial YBCO thin films are used so that grain boundaries do not play a role.

3.1. Experimental set-up and techniques

Coplanar thin film resonators (central conductor width $w = 100$ μm , distance of ground planes $a = 180$ μm , resonant frequency $f_0 = 1.4$ GHz) were patterned from epitaxial YBCO films (thickness $d \approx 300$ nm) on sapphire substrates. Various similar descriptions of the rf current density profile in superconducting coplanar structures exist in literature. For the analysis of our experiments, the approximation of the superconductor using an ideal conductor with artificial cut-offs is taken [20]:

$$j_z(x) = \frac{I}{wK(w/a)} \times \begin{cases} [(1 - (2x/w)^2)(1 - (2x/a)^2)]^{-1/2} & \text{for } |x| < \frac{w}{2} - \lambda \\ [(1 - (w/a)^2)\lambda/w]^{-1/2} & \text{for } \frac{w}{2} - \lambda < |x| < \frac{w}{2}. \end{cases} \quad (1)$$

Here, λ is the London penetration depth and $K(w/a)$ the complete elliptic integral, which for our geometry is $K \approx 1.72$. Due to this characteristic current distribution (see the inset of figure 3) the values for the power handling capability and,

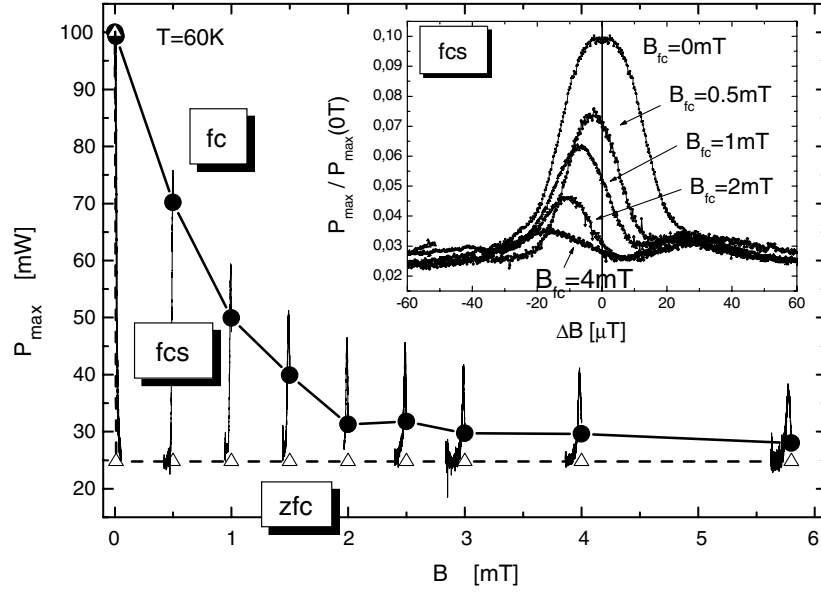


Figure 1. The dc field dependence of the power handling capability of coplanar YBCO resonators for field cooled (fc, solid circles), zero field cooled (zfc, open triangles) and field cooled sweep (fcs, solid lines) experiments. The inset shows the fcs measurement starting at different fields B_{fc} on a normalized scale as a function of field sweep ΔB .

consequently, of the dissipated power are relatively small so that thermal effects are limited to values $\Delta T < 30 \mu\text{K}$ and can therefore be neglected [21].

The resonators were measured in an He flow cryostat. An additional dc magnetic field of $-0.6 \text{ T} < B < 0.6 \text{ T}$ was applied parallel to the c -axis of the sample, i.e. normal to the sample surface (in the following this field will be called the dc magnetic field). The loaded quality factor of the resonator Q_L and S -parameters were measured in the frequency domain using a network analyser (HP8720D). The power handling capability P_{max} is defined by the oscillating microwave power $P_{\text{osc}} = Q_L P_{\text{in}}$ at which the unloaded quality factor $Q_0 = Q_L(1 - S_{11} - S_{21})^{-1}$ is degraded to 80% of its low-power value, i.e. $Q_0(P_{\text{max}}) = 0.8Q_0(P \rightarrow 0)$ with $Q_0 \approx 20.000\text{--}30.000$ in the limit $P \rightarrow 0$ and $T \rightarrow 0$.

Since the rf current is strongly peaked at the edge of the central conductor, these devices turn out to be highly sensitive to magnetization or vortex penetration. Thus, the power handling capability can be analysed locally via establishing various distributions of magnetic flux in the device. For this purpose, the dc magnetic field was applied in field cooled (fc), zero field cooled (zfc), and field cooled sweep (fcs) experiments. In fc and zfc experiments the resonator was cooled to the superconducting state in an applied dc magnetic field or in zero field, respectively. In fcs experiments, the sample was first cooled to the superconducting state in an applied dc field B_{fc} (where the field cooled state is established) and, subsequently, the dc field was swept or cycled around B_{fc} .

3.2. Experimental results

Figure 1 represents an overview of the power handling capability as a function of the dc magnetic field of a typical coplanar resonator in fc, zfc and fcs experiments. The power handling capability P_{max} depends strongly upon the way the dc magnetic field is established. For fc

experiments, a homogeneous vortex distribution is frozen into the superconductor. The linear increase of the vortex density in the resonator as function of dc magnetic field results in a gradual decrease of the power handling capability. In contrast, in the zfc case, vortex penetration into the field-free superconductor occurs primarily in regions close to the edge of the central conductor where the vortices are pinned. Thus, the maximum of this resulting extremely inhomogeneous vortex distribution coincides with the maximum of the microwave current distribution (see the inset of figure 3), resulting in a strong reduction of P_{max} even at extremely small dc fields (of a few microtesla). The following quite constant power handling capability at larger dc fields ($|B| > 25 \mu\text{T}$) is consistent with observations of a shift of the flux front into the superconductor [22]. Since the interior of the superconductor does not carry large rf currents, this shift does not seriously affect the power handling capability. At larger dc magnetic fields, the fc and zfc values of P_{max} seem to merge.

For fcs experiments the resulting dc field dependence of the power handling capability (see the inset of figure 1) represents a fingerprint of the processes of magnetization and vortex penetration. Although, in fcs experiments, we can see an increase of the power handling capability as a function of the dc magnetic field, this behaviour is qualitatively and quantitatively different from an ‘anomalous’ dc magnetic field dependence of R_s that has been reported earlier [24]. It can be understood by considering the effective dc magnetic field at the superconductor surface

$$B_{\text{eff}} = B_{fc} + s \Delta B. \quad (2)$$

For dc field changes ΔB , demagnetizing effects have to be taken into account. A demagnetizing factor D leads to an effective magnetic field $H_{\text{eff}} = H_0/(1 - D) = sH_0$ at the surface of a field-free superconductor, where H_0 is the externally applied magnetic field and $s = (1 - D)^{-1}$. For thin films with perpendicular magnetic field $s \gg 1$.

In fcs experiments (see the inset of figure 1) for small dc field changes $\Delta B < 10 \mu\text{T}$, the superconductor is magnetized, as we have demonstrated by reversible behaviour in field-cycling experiments [25]. In this case, the B_{eff} decays on the scale of λ at the superconductor surface, and no penetration of vortices takes place. For $\Delta B > 0$, the frozen-in magnetic field at the superconductor surface is increased, and therefore a decrease of the power handling capability is observed. For $\Delta B < 0$, the frozen-in magnetic field B_{fc} is compensated by $s\Delta B$, and thus an increase of the power handling capability is achieved. The maximum power handling capability is reached upon total field compensation at the edge of the superconductor $B_{\text{eff}} = 0$. From this condition, the field enhancement factor $s \approx 185$ could be determined experimentally, in agreement with theoretical expectations [21]. Only for larger amplitudes $|\Delta B| > 10 \mu\text{T}$ could irreversible behaviour be observed in dc field cycling experiments, indicating the onset of penetration and pinning of vortices inside the superconductor [25]. For $\Delta B > 10 \mu\text{T}$ vortices and for $\Delta B < -10 \mu\text{T}$ anti-vortices nucleate in the superconductor, contributing to the asymmetry of P_{max} as function of ΔB . The small side peaks observed in the inset of figure 1 can be explained by a relaxation of the magnetization upon vortex penetration.

Thus we can state that the power handling capability in dc magnetic fields is strongly affected by (i) the magnetization of the superconductor, (ii) vortex penetration and pinning, and (iii) the vortex density distribution.

3.3. Modelling of the experimental results

In the following, the dc field dependence of P_{max} will be discussed in terms of a new model that considers (i) a superposition and (ii) a limitation of the current density in the superconductor. Ambient dc magnetic fields cause screening currents in the superconductor with contributions j_M due to the magnetization at the edge of the sample and j_V due to vortices inside the superconductor. Both currents superimpose to the rf current density j_{rf} , yielding a total local current density $j_{\text{tot}} = j_{\text{rf}} + j_M + j_V$ in the coplanar resonator. A nonlinearity of the system implies that the total power and thus the local current density is limited by a maximum value $j_{\text{tot}} < j_{\text{max}}$ defining the limit of the linear regime. Assuming that screening currents effectively reduce the maximum transportable rf current, we can approximate

$$j_{\text{max}}(B, x) = j_{\text{max}, B=0}(x) - j_M(B, x) - j_V(B, x). \quad (3)$$

This model automatically yields a power handling capability that strongly depends on the kind of dc magnetization experiment, i.e., fc, zfc or fcs.

3.3.1. Field cooled experiments: the impact of vortices.

In fc experiments a homogeneous distribution of vortices in the superconductor can be assumed and magnetization effects can be neglected for not too small fields, i.e., $j_{\text{tot}} \approx j_{\text{rf}} + j_V$. We assume an ideal vortex lattice with each vortex effectively reducing the rf current on a width of the order $\alpha\lambda_{\text{eff}}$ around its position x_n with the effective London penetration depth λ_{eff} and α of the order 1. The maximum total current I_{tot} can be calculated from the experimentally determined rf current $I_{\text{rf}, \text{max}} = (2P_{\text{max}}/Z_L)^{1/2}$ by a summation of the individual

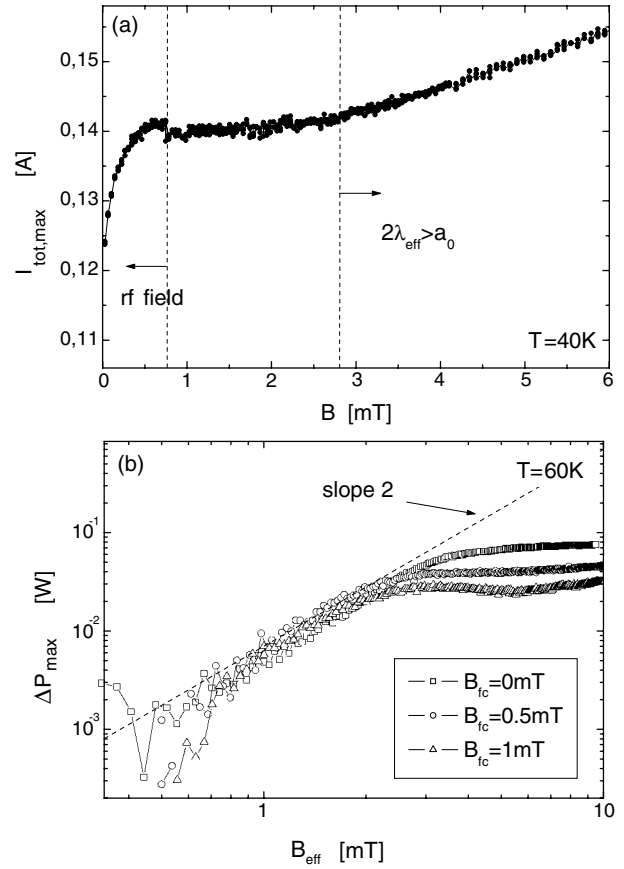


Figure 2. (a) The dc field dependence of the calculated total current (equation (5)) in fc experiments. The values for the rf self-field and the onset of overlap and compensation of vortex screening currents are marked and restrict the validity of equation (5) and thus the regime of constant total current. (b) ΔP_{max} as a function of the effective dc magnetic field B_{eff} for field sweep experiments (zfc and fcs) for different values of the frozen-in dc magnetic field B_{fc} .

screening currents of the vortices within the cross section of the central conductor [25]:

$$I_{\text{tot}, \text{max}} = I_{\text{rf}, \text{max}} + \sum_{\text{Vortices } n} j_z(x_n) 2\lambda_{\text{eff}} \alpha. \quad (4)$$

Using equation (1) yields the maximum total current:

$$I_{\text{tot}, \text{max}} = I_{\text{rf}, \text{max}} \left(1 + \frac{\lambda_{\text{eff}} \alpha}{w K(w/a)} \times \sum_{\text{Vortices } n} 2 \left(\left[1 - \left(\frac{2x_n}{w} \right)^2 \right] \left[1 - \left(\frac{2x_n}{a} \right)^2 \right] \right)^{-0.5} \right). \quad (5)$$

Figure 2(a) shows the dc field dependence of the maximum total current for a set of fc experiments on a typical resonator. The transformation of the rf current via equation (5) to the total current demonstrates the expected field independence of $I_{\text{tot}, \text{max}}$ for a dc magnetic field range between 0.5 and 3 mT. Deviation from the field independence can be explained at low fields by the effect of the rf field itself, which can be approximated to $B_{\text{rf}} \approx \mu_0 I_{\text{rf}} / 2w \approx 0.88 \text{ mT}$ using the experimental value $I_{\text{rf}} \approx 0.14 \text{ A}$. At large dc fields ($B_{\text{fc}} > 3 \text{ mT}$), vortices start to overlap $a_0 \leq 2\lambda_{\text{eff}}$ resulting in an overestimation of the total current by equation (5).

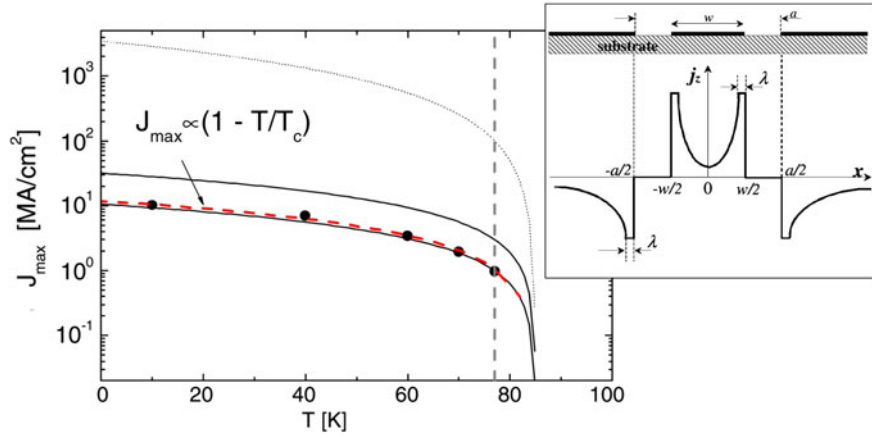


Figure 3. A comparison of the temperature dependence of the maximum rf current density for a coplanar YBCO resonator (dots) with typical values for the dc critical current densities j_c expected for depinning (solid curves) and pair-breaking critical current (dotted curves). The inset shows the rf current density distribution across the resonator cross section.

3.3.2. *Field sweep experiments: the impact of the magnetization.* Restricting our consideration to small field changes ΔB in dc magnetic field sweep experiments (see figure 2(a)), the penetration of vortices additional to those that are frozen in during cooling in the dc field B_{fc} can be neglected and, thus, $j_{tot} \approx j_{rf} + j_M$. Let us now consider the case of zfc and fcs experiments for increasing field. The effective dc field B_{eff} (equation (2)) decays exponentially at the superconductor surface and, according to our model, the associated screening current density j_M reduces the transportable rf current. Thus the power handling capability is reduced according to [25]:

$$\Delta P_{max} = P_{max}(B_{eff}) - P_{max}(B_{fc}) \propto (j_M(0)\lambda_{eff}t)^2 \propto B_{eff}^2. \quad (6)$$

The double-logarithmic plot (figure 2(b)) of ΔP_{max} as a function of effective dc magnetic field B_{eff} for a typical set of zfc and fcs experiments demonstrates the excellent agreement of the data with the predicted dc magnetic field dependence in equation (6). At larger dc fields, starting at $B_{eff} \approx 2-3$ mT, a deviation from the quadratic dependence is observed, which can be attributed to the onset of vortex penetration. The value of $B_{eff} \approx 2-3$ mT agrees with the geometrical barrier for vortex tunnelling $H_t = H_{c1}t/w$ for our geometry [23].

3.3.3. *Zero field experiments.* Finally, zero dc field measurements are discussed in terms of our model. Generally the rf current density profile shows a maximum at the edges of the superconducting resonator. According to equation (1), the maximum current density can be calculated from the experimentally determined power handling capability P_{max} :

$$j_{rf,max} = \frac{\sqrt{2P_{max}}}{K(w/a)} [Z\lambda_{eff}wt^2(1 - (w/a)^2)]^{-1/2}. \quad (7)$$

Figure 3 shows the resulting temperature dependence of $j_{rf,max}$ for a typical YBCO resonator. Two interesting aspects should be noted: (i) $j_{rf,max}$ increases linearly with temperature, and (ii) the order of magnitude of $j_{rf,max}$ agrees with typical values for the dc critical current density of YBCO, e.g. at 77 K $1 \text{ MA cm}^{-2} < j_{rf,max} < 3 \text{ MA cm}^{-2}$ [11]. In contrast, the experimentally observed maximum rf current density is about two orders of magnitude smaller than the pair-breaking current

density. Thus, we conclude that the power handling capability in these weak link free samples (see section 2.3) in zero field seems to be limited by the dc critical current density.

4. Conclusions

In summary, we have presented a set of new experiments in which we examine the power handling capability of HTS thin film resonators in additionally applied dc magnetic fields in field cooled and field sweep experiments. The careful analysis of our experiments shows that (i) the microwave properties depend on magnetization and vortex distribution, (ii) the power handling and quality factor of the devices are strongly affected by the way the dc magnetic field is approached, and (iii) the microwave power handling can be understood in terms of a simple model that considers all contributions to the current density in the superconductor and is based on a limitation of the total current density. All experiments in static and swept dc magnetic fields as well as in zero magnetic field could be consistently described using the proposed model for the power handling capability. The limiting value for the current density agrees in magnitude and temperature dependence with typical values for the dc critical current density.

In conclusion, in the search for the so-called fundamental limiting mechanism we have found strong experimental evidence that the mechanism that limits the power handling capability in HTSs is current driven, and that the limiting scale for the onset of nonlinear microwave effects in the absence of large-angle grain boundaries seems to be given by the dc critical current density J_c .

Acknowledgments

We acknowledge helpful discussions with N Klein, M Hein, E H Brandt, D E Oates. This work has been supported by the ESF Vortex programme.

References

- [1] Lahl P and Wördenweber R 2001 *Appl. Phys. Lett.* **79** 512
- [2] Booth J C, Vale L R and Ono R H 2001 *Physica C* **357-360** 1516
- [3] Zaitsev A G *et al* 2001 *Appl. Phys. Lett.* **79** 4174

- [4] Hu W *et al* 1999 *Appl. Phys. Lett.* **75** 2824
- [5] Claassen J H *et al* 1999 *Supercond. Sci. Technol.* **12** 714
 Claassen J H *et al* 1999 *Appl. Phys. Lett.* **74** 4023
- [6] Dahm T and Scalapino D J 1996 *Appl. Phys. Lett.* **69** 4248
- [7] Dahm T and Scalapino D J 1997 *J. Appl. Phys.* **81** 2002
- [8] Oates D E *et al* 2004 *Supercond. Sci. Technol.* **17** S290–4
- [9] Dahm T *et al* 1999 *J. Supercond.* **12** 339
- [10] Willemsen B A *et al* 1998 *Phys. Rev. B* **58** 6650
- [11] Dam B *et al* 1999 *Nature* **399** 439
- [12] Hylton T L *et al* 1988 *Appl. Phys. Lett.* **53** 1343
- [13] Dimos D *et al* 1990 *Phys. Rev. B* **41** 4038
- [14] Nguyen P P *et al* 1993 *Phys. Rev. B* **48** 6400
- [15] Nguyen P P *et al* 1995 *Phys. Rev. B* **51** 6686
- [16] Habib Y M *et al* 1998 *Phys. Rev. B* **57** 13833
- [17] Habib Y M *et al* 1998 *Appl. Phys. Lett.* **73** 2200
- [18] Xin H *et al* 2002 *Phys. Rev. B* **65** 214533
- [19] Halbritter J 2003 *Supercond. Sci. Technol.* **16** R47
- [20] Vendik J B *et al* 1996 *Superconductor Microwave Technology*
 part II. *Superconducting Microwave Circuits*
- [21] Lahl P 2001 *PhD Thesis* Verlag Forschungszentrum Jülich,
 Germany
- [22] Pannetier M *et al* 2003 *Phys. Rev. B* **67** 212501
- [23] Zeldov E *et al* 1994 *Phys. Rev. Lett.* **73** 1428
- [24] e.g. Velichko A V *et al* 2002 *Phys. Rev. B* **65** 104522
 Jin B B *et al* 1999 *Physica C* **316** 224
- [25] Lahl P and Wördenweber R 2002 *Appl. Phys. Lett.* **81** 505